

Identification of Genes Modulated in Rheumatoid Arthritis Using Complementary DNA Microarray Analysis of Lymphoblastoid B Cell Lines From Disease-Discordant Monozygotic Twins

Christian S. Haas,¹ Chad J. Creighton,¹ Xiujun Pi,¹ Ira Maine,¹ Alisa E. Koch,¹ G. Kenneth Haines, III,² Song Ling,¹ Arul M. Chinnaiyan,¹ and Joseph Holoshitz¹

Objective. To identify disease-specific gene expression profiles in patients with rheumatoid arthritis (RA), using complementary DNA (cDNA) microarray analyses on lymphoblastoid B cell lines (LCLs) derived from RA-discordant monozygotic (MZ) twins.

Methods. The cDNA was prepared from LCLs derived from the peripheral blood of 11 pairs of RA-discordant MZ twins. The RA twin cDNA was labeled with cy5 fluorescent dye, and the cDNA of the healthy co-twin was labeled with cy3. To determine relative expression profiles, cDNA from each twin pair was combined and hybridized on 20,000-element microarray chips. Immunohistochemistry and real-time polymerase chain reaction were used to detect the expression of selected gene products in synovial tissue from patients with RA compared with patients with osteoarthritis and normal healthy controls.

Results. In RA twin LCLs compared with healthy co-twin LCLs, 1,163 transcripts were significantly differentially expressed. Of these, 747 were overexpressed and 416 were underexpressed. Gene ontology analysis revealed many genes known to play a role in apoptosis, angiogenesis, proteolysis, and signaling. The 3 most significantly overexpressed genes were laeverin (a novel enzyme with sequence homology to CD13), 11 β -hydroxysteroid dehydrogenase type 2 (a steroid pathway enzyme), and cysteine-rich, angiogenic inducer 61 (a known angiogenic factor). The products of these genes, heretofore uncharacterized in RA, were all abundantly expressed in RA synovial tissues.

Conclusion. Microarray cDNA analysis of peripheral blood-derived LCLs from well-controlled patient populations is a useful tool to detect RA-relevant genes and could help in identifying novel therapeutic targets.

Supported in part by the NIH (grants AI-47331, AR-46468, AR-20557, AR-48310, AI-40987, HL-58694, and AR-48267), the Arthritis Foundation (Biomedical Research Grant), and the Office of Research and Development, Department of Veterans Affairs. Dr. Haas' work was supported by a postdoctoral training grant from the American Heart Association (AHA0423758Z). Mr. Creighton's work was supported by the University of Michigan Cancer Biology Training Program. Dr. Pi's work was supported by a postdoctoral training grant from the NIH (AR-07080). Dr. Koch is an incumbent of the Frederick G. L. Heutwell and William D. Robinson Professorial Chair in Rheumatology.

¹Christian S. Haas, MD, Chad J. Creighton, BSc, Xiujun Pi, MD, PhD, Ira Maine, PhD, Alisa E. Koch, MD, Song Ling, PhD, Arul M. Chinnaiyan, MD, PhD, Joseph Holoshitz, MD: University of Michigan Medical Center, Ann Arbor; ²G. Kenneth Haines, III, MD: Northwestern University Feinberg Medical School, Chicago, Illinois.

Dr. Haas and Mr. Creighton contributed equally to this work.

Address correspondence and reprint requests to Joseph Holoshitz, MD, 5520D MSRB1, Box 0680, University of Michigan, 1150 West Medical Center Drive, Ann Arbor, MI 48109-0680. E-mail: jholo@umich.edu.

Submitted for publication December 1, 2005; accepted in revised form March 30, 2006.

Rheumatoid arthritis (RA) is a chronic inflammatory joint disease. Neither the pathogenesis of RA nor its etiology is fully understood. The inflamed synovium is characterized by infiltration of inflammatory cells, the presence of lymphocytes, formation of new blood vessels, and hyperplasia of synovial lining cells that release proteolytic enzymes, leading to destruction of adjacent cartilage and bone (for review, see ref. 1). It has previously been postulated that aberrant angiogenesis, impaired apoptosis, and migration of cells from the peripheral blood into the synovial compartment may collaboratively contribute to the formation and propagation of rheumatoid pannus (2,3). Increasing evidence over the past several years indicates that B lymphocytes play a central role in RA pathogenesis. These cells appear to home to the pannus from the peripheral blood

and form germinal center–like structures in the inflamed synovium. They are believed to release cytokines, engage in antigen presentation, sustain cell survival, and enhance pannus growth.

Susceptibility to RA has a strong heritable component, with several genes implicated, both within and without the HLA complex (4). Interestingly, despite the strong involvement of genetic factors, occurrence of the disease among genetically susceptible individuals seems to be random, as evidenced by the high disease discordance rate among monozygotic (MZ) twins. Meta-analysis of the literature revealed that the rate of concordance of RA among these genetically identical twins is only ~15% (5). This low concordance rate suggests that although susceptibility to RA depends on genetic factors, disease pathogenesis may involve nonheritable mechanisms.

To identify disease-associated genes regulated by nongenetic or epigenetic mechanisms, we compared gene expression profiles in immortalized lymphoblastoid B cell lines (LCLs) from RA-discordant MZ twins. A total of 1,163 transcripts, representing 827 uniquely named genes, were differentially expressed in RA twins relative to their healthy cotwins, including 747 overexpressed and 416 underexpressed transcripts. Many of the identified genes have been previously implicated in RA and segregated into several discrete RA-relevant functional categories. The 3 most significantly overexpressed genes, which belong, respectively, to the proteolytic, inflammatory, and angiogenic functional categories, have not been previously implicated in RA. This study is the first to demonstrate that the products of these 3 genes are abundantly expressed in RA pannus.

PATIENTS AND METHODS

Cell lines and synovial tissues. LCLs were prepared from the peripheral blood B cells of 11 pairs of RA-discordant MZ twins, using a standard Epstein-Barr virus (EBV) transformation technique (6). LCLs were cultured in supplemented RPMI 1640 containing 10% heat-inactivated fetal bovine serum (FBS; Irvine Scientific, Santa Ana, CA) at a density of $0.5\text{--}1.0 \times 10^6$ cells/ml. All lines had been maintained in identical tissue culture conditions, cell density, and viability. LCLs were kept in continuous long-term (2–6-month) culture, with no measurable change in their viability or functional properties over time. Aliquots of paired LCLs were periodically frozen, and these samples were occasionally used in rare instances of culture loss. In those instances, the most recently frozen samples of both the RA twin LCLs and the healthy cotwin LCLs were thawed at the same time to assure identical tissue culture history.

Synovial tissue was obtained from patients with RA or patients with osteoarthritis (OA) at the time of arthroplasty or synovectomy. All patients fulfilled the American College of Rheumatology (formerly, the American Rheumatism Association) criteria for either RA or OA (7,8). Normal synovial tissue was obtained from fresh samples at autopsy or from amputations. All samples were obtained with institutional review board consent. The synovial tissue was either used freshly to prepare RNA or embedded in optimal cutting temperature compound (Sakura Finetek, Torrance, CA) and frozen at -80°C until used.

Extraction of total RNA and reverse transcription.

Total cellular RNA was extracted with the RNeasy Mini Kit (Qiagen, Valencia, CA). Briefly, 1×10^7 line cells or 50–100 mg of homogenized synovial tissue was lysed in 300 μl of buffer containing 4M guanidinium salt and β -mercaptoethanol, and homogenized by using a microultrasonic cell disrupter. After addition of 300 μl of 70% ethanol, the mixture was loaded onto the RNeasy spin column and centrifuged for 0.5 minutes at 8,000g. The column was washed with a buffer containing 70% ethanol and centrifuged twice. After treatment with DNase I, total RNA was collected with 50 μl of diethyl pyrocarbonate–treated water and stored at -80°C . The concentration and purity of RNA were determined by measuring the absorbance at 260 nm and 280 nm, respectively. Complementary DNA (cDNA) was synthesized from 1 μg total RNA by using Multiscribe Reverse Transcriptase (Applied Biosystems, Foster City, CA). Negative control samples were prepared using all reagents except the RNA sample and without the reverse transcription step.

Microarrays. Microarrays (20,000-gene chip, or 20K cDNA array) containing sequence-verified polymerase chain reaction (PCR)–amplified human cDNA were manufactured as described previously (9). (The clone information is available online at <http://www.pathology.med.umich.edu/chinnaiyan/index.html>. Protocols for printing and postprocessing of arrays are available online at <http://www.microarrays.org/protocols.html>.) Complementary DNA microarray analysis of gene expression was done essentially as described previously (9). Briefly, total RNA isolated from the twins with RA was reverse transcribed and labeled with cy5 fluorescent dye. RNA from the healthy cotwins was prepared in a similar manner and labeled with cy3 fluorescent dye. The labeled products were then mixed and hybridized to 20K cDNA array. For each profile, the RA twin RNA in the cy5 channel was paired with RNA in the cy3 channel from the corresponding disease-free twin. The images were flagged and normalized using the Genepix software package (Axon Instruments, Union City, CA). Significance of gene expression (expressed as a *q* value) was determined using significance analysis of microarrays (SAM) (10). Gene expression patterns were visualized as colorgrams using TreeView (11). Gene ontology (12) annotation term assignments were obtained from LocusLink (13).

Immunohistochemistry. Immunohistochemistry was performed on human synovial tissues for cysteine-rich, angiogenic inducer 61 (Cyr61) with polyclonal rabbit antibody, cross-reacting with the human, mouse, and rat protein (Santa Cruz Biotechnology, Santa Cruz, CA), and for 11 β -hydroxysteroid dehydrogenase type 2 (11 β -HSD2) with polyclonal sheep anti-human antibody (The Binding Site, Birmingham, UK). Cryosections (5 μm) were fixed in cold acetone for

20 minutes. Endogenous peroxidase was quenched by treatment with 3% H₂O₂ for 5 minutes. Synovial tissue was pretreated with 3% FBS for 1 hour at 37°C before application of the primary antibody at a final concentration of 1 µg/ml (for Cyr61) or 69 µg/ml (for 11β-HSD2). Indirect immunoperoxidase staining was performed using Vector Elite ABC kits (Vector, Burlingame, CA) and diaminobenzidine (Kirkegaard and Perry, Gaithersburg, MD) as a chromogen, followed by counterstaining with hematoxylin. Rabbit and sheep IgG were used as negative controls. Staining patterns were analyzed, and representative sections were photographed.

Double immunofluorescence was performed on human synovial tissue to determine colocalization of Cyr61 with B cells, using CD20 as a B cell marker. After fixation with ice-cold acetone for 10 minutes and blocking with 3% horse serum, fluorescein isothiocyanate-conjugated anti-human CD20 antibody (BD PharMingen, San Diego, CA) was added at a dilution of 1:100 in phosphate buffered saline and incubated at 4°C overnight. Goat anti-Cyr61 antibody (1 µg/ml) or an IgG control was added for 1 hour at room temperature. As secondary antibody, Alexa Fluor 555 donkey anti-goat IgG (Molecular Probes, Eugene, OR) was used at a dilution of 1:200 at room temperature for 30 minutes. Images were obtained using an Olympus BX51 fluorescence microscope system with DP Manager imaging software (Olympus, Melville, NY).

Microscopic analysis. Various synovial tissue cell types were evaluated for Cyr61 and 11β-HSD2 staining, and included lining cells, macrophages, endothelial cells, smooth muscle cells, and fibroblasts. Cell types were distinguished based on their morphologic characteristics, as previously described (14). Immunostaining was evaluated and graded in a blinded manner. Immunopositivity was determined using the following scoring system: 0 = no staining; 1 = few scattered positive cells; 2 = moderate number of stained cells; 3 = large number of positive cells; 4 = very heavy/dense population of immunoreactive cells. The inflammation score was obtained using the following scoring system: 0 = normal; 1 = increased number of inflammatory cells, arrayed as individual cells; 2 = moderate number of inflammatory cells; 3 = increased number of inflammatory cells, including distinct clusters (aggregates); 4 = marked diffuse infiltrate of inflammatory cells (14). Synovial tissue vascularity was scored on a 1–4 scale as follows: 1 = marked decrease in blood vessels; 2 = normal vessel density; 3 = increased vessel density; 4 = marked increase in vessel density.

Quantification of laeverin messenger RNA (mRNA) expression in synovial tissue by real-time PCR. Exon-spanning primers and probes for laeverin were designed according to published cDNA sequences of the human gene (NM_173800). The forward primer was 5'-AAGAAAAGATTCAA-CTTGCTTATGCA-3', the reverse primer was 5'-TGGAGATGTGCTGATGGCATAAC-3', and the probe was 5'-FAM-CTGCAGCAAAGACCCATGGATACTTAAC-AGA-TAMRA-3'. The PCR product was 92 bp from cDNA and 300 bp from genomic DNA. Laeverin mRNA levels were normalized against β-actin (NM_001101), using a forward primer (5'-TTGCCGACAGGATGCAGAA-3'), a reverse primer (5'-GCCGATCCACACGGAGTACT-3'), and a probe (5'-FAM-CCCTGGCACCCAGCACAATGAAG-TAMRA-3'). The PCR product was 101 bp from cDNA and 213 bp from genomic DNA.

PCR was carried out with 2× PCR MasterMix (Applied Biosystems) in a total volume of 50 µl containing 5 µl (2 µl for β-actin) of cDNA, 0.4 µM of each PCR primer, 0.2 µM of Taqman probe with passive reference, and 25 µl PCR MasterMix. Laeverin and β-actin genes were amplified in duplicate in separate tubes. The amplification parameters were 50°C for 2 minutes, 95°C for 10 minutes, and 50 cycles of 95°C for 15 seconds and 60°C for 1 minute. The fluorescence emission from individual PCR tubes at each cycle was monitored in a 7300 Real-Time PCR system (Applied Biosystems). The cycle threshold of detection (C_t) values were defined as corresponding to the PCR cycle number at which the fluorescence was detectable above an arbitrary threshold, based on baseline data within cycles 3–15. The arbitrary threshold was decided to ensure that the C_t values were obtained in the exponential phase of the PCR, during which there are no rate-limiting components.

To construct a standard curve, cDNA was synthesized from total RNA extracted from cell culture, and then diluted (from 2 times to 32 times) in 5 steps. A standard curve of C_t values against the log value of cDNA was generated for both laeverin and β-actin. The relative concentrations of laeverin and β-actin were obtained from the standard curve, and the ratios of laeverin normalized against β-actin were calculated.

Statistical analysis. Immunohistochemical analysis and PCR results are expressed as the mean ± SEM. Data were analyzed using Student's *t*-test when applicable. *P* values less than 0.05 were considered significant. Pearson's correlation coefficients were calculated to determine the relationship between inflammation and Cyr61 or 11β-HSD2 staining. The significance of these correlations was determined using analysis of variance. Microarray data were analyzed using SAM, performed as described above.

RESULTS

To identify non-hereditarily determined mRNA expression patterns in RA, we performed cDNA microarray analysis in LCLs derived from 11 pairs of RA-discordant MZ twins. RNA samples from all RA twins were labeled with cy5, whereas paired RNA samples from the healthy cotwins were labeled with cy3. The labeled RNA was then hybridized on 20,000-gene DNA microarray chips designed to measure human mRNA. Analysis of the microarray data by SAM (10) revealed numerous differences in gene expression between the RA twins and their healthy cotwins. SAM provides an estimate of the number of genes that may appear differentially expressed due to chance alone.

At an expected false-discovery rate of 5%, a total of 1,163 mRNA transcripts (827 uniquely named genes) showed significant overexpression or underexpression in the RA twins compared with their healthy cotwins

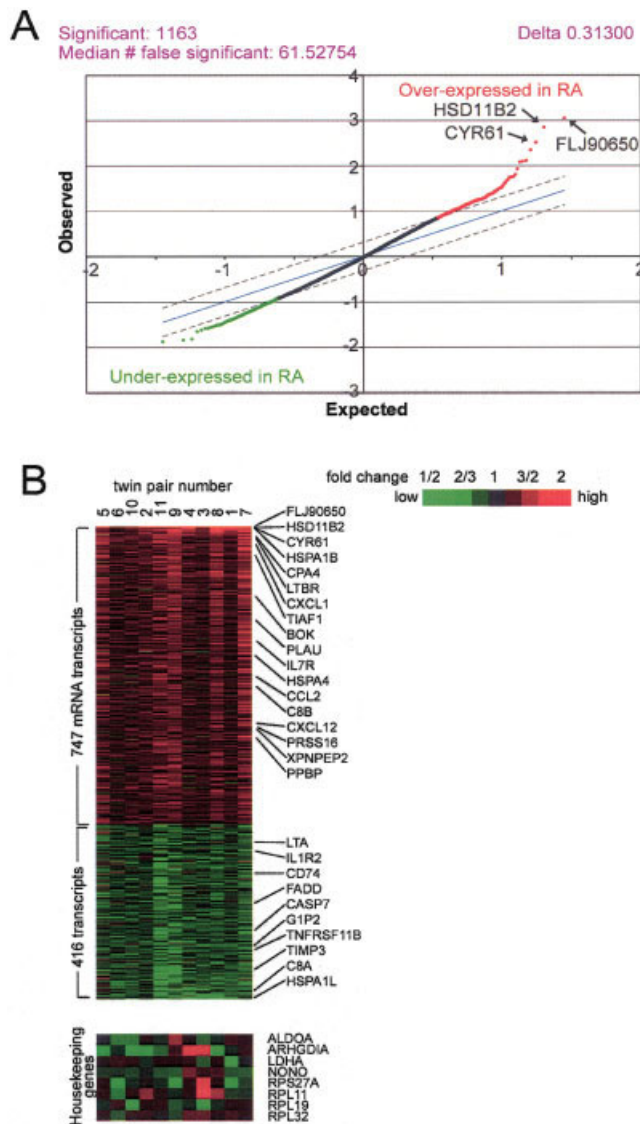


Figure 1. Complementary DNA microarray analysis of lymphoblastoid B cell lines from 11 rheumatoid arthritis (RA)-discordant monozygotic (MZ) twin pairs. **A**, Significance analysis of microarrays (SAM) assessing gene expression profiles for 1,163 mRNA transcripts demonstrates significant gene overexpression or underexpression in RA patients compared with their corresponding arthritis-free MZ twins (false-discovery rate 5%). **B**, Expression colorgram for 1,163 mRNA transcripts demonstrates significant up- or down-regulation of mRNA in RA samples relative to healthy cotwin samples. Each row represents a gene; each column represents a twin pair. The level of relative expression of each gene in each twin pair is represented using a red-to-green color scale (as shown in the key); gray indicates missing data. Genes are ordered by significance of expression as determined by SAM analysis. Representative genes are annotated. For reference, expression values for well-known housekeeping genes are also shown.

(Figures 1A and B). Of the 747 genes overexpressed in the RA twins, the 3 most significant ones were *FLJ90650* (for the hypothetical protein recently identified as laeverin [15]), *HSD11B2* (for 11β -HSD2), and *CYR61* (for Cyr61). Significantly reduced expression in the RA twins compared with their healthy cotwins was found for 416 transcripts. Table 1 lists the transcripts that were most significantly ($q < 0.012$) over- or underexpressed in the RA twins compared with their healthy cotwins.

The group of 1,163 over- or underexpressed transcripts was analyzed for functional clusters, using the gene ontology annotations (12). We preselected gene ontology categories of particular relevance to RA. Many genes with gene ontology annotations known to be involved in RA pathogenesis were differentially expressed in the twins' LCLs (Tables 2 and 3). Of particular relevance, several proapoptotic genes (e.g., *CASP7*, *FADD*) were found to be underexpressed, while some antiapoptotic genes (e.g., *TIAF1*) were overexpressed. Other RA-relevant categories of genes included immune response genes, proteolysis and peptidolysis genes, heat-shock protein genes, and chemokine and chemokine receptor genes (Tables 2 and 3).

To assess the relevance of the differentially expressed genes in RA, we sought to determine whether products or transcripts of the 3 most overexpressed genes (*FLJ90650*, *CYR61*, and *HSD11B2*) could be detected in the synovium. Figure 2A shows the results of immunohistochemical analysis of Cyr61 protein expression in synovial tissue from RA and OA patients and from normal healthy individuals. As can be seen in Figure 2B, RA synovial tissue showed significant overexpression of Cyr61 on synovial macrophages (mean \pm SEM staining score 2.9 ± 0.1) compared with normal (staining score 1.3 ± 0.2 ; $P = 2.3 \times 10^{-7}$) and OA (staining score 1.8 ± 0.2 ; $P = 2 \times 10^{-4}$) synovial tissue. Increased Cyr61 immunoreactivity was also found on RA synovial tissue lining cells (staining score 3.3 ± 0.2) as compared with normal (staining score 2.2 ± 0.5 ; $P = 0.010$) and OA (staining score 2.6 ± 0.2 ; $P = 0.005$) synovial tissue lining cells. In OA synovial tissue, a significant increase in Cyr61 expression in endothelial cells (staining score 1.3 ± 0.2) was found, which clearly distinguished OA synovial tissue from normal synovial tissue (staining score 0.4 ± 0.2 ; $P = 0.002$) and RA synovial tissue (staining score 0.6 ± 0.2 ; $P = 0.007$). Of interest, Cyr61 in RA synovial tissue appeared to be down-regulated in both smooth muscle cells and fibroblasts relative to these expression levels in normal and OA synovial tissue. Thus, the lineage-specific expression

Table 1. Top-named genes differentially expressed in twins with rheumatoid arthritis (RA) compared with their healthy cotwins*

Expression, image no.	Gene	Title
Overexpressed in RA twins		
767642	<i>FLJ90650</i>	Laeverin
415145	<i>HSD11B2</i>	11 β -hydroxysteroid dehydrogenase 2
378488	<i>CYR61</i>	Cysteine-rich, angiogenic inducer 61
811813	<i>HSPA1B</i>	Heat shock 70-kd protein 1B
739221	<i>FLJ20473</i>	Hypothetical protein
666059	<i>MX1</i>	Myxovirus (influenza virus) resistance 1
687393	<i>PI4KII</i>	Phosphatidylinositol 4-kinase type II
742930	<i>KIAA0804</i>	KIAA0804 protein
361255	<i>SLC17A5</i>	Solute carrier family 17 (anion/sugar transporter), member 5
282663	<i>OSTF1</i>	Osteoclast stimulating factor 1
320865	<i>FLJ30532</i>	Hypothetical protein
307660	<i>FABP4</i>	Fatty acid binding protein 4, adipocyte
306421	<i>BBF2H7</i>	Basic transcription factor 2
223661	<i>FRZB</i>	Frizzled-related protein
244703	<i>ITGBL1</i>	Integrin β -like 1 (with EGF-like repeat domains)
359285	<i>CPA4</i>	Carboxypeptidase A4
282501	<i>SLC6A12</i>	Solute carrier family 6 (neurotransmitter transporter), member 12
811900	<i>LTBR</i>	Lymphotoxin- β receptor
129112	<i>PAPPA</i>	Pregnancy-associated plasma protein A
503819	<i>PRELP</i>	Proline arginine-rich end leucine-rich repeat protein
811874	<i>JPH1</i>	Junctophilin 1
758314	<i>MGC13047</i>	Hypothetical protein
198874	<i>FLJ10922</i>	Hypothetical protein
731054	<i>MTP</i>	Microsomal triglyceride transfer protein
Underexpressed in RA twins		
40699	<i>PPP2R2B</i>	Protein phosphatase 2, regulatory subunit B (PR 52), β -isoform
33511	<i>SLMAP</i>	Sarcolemma-associated protein
205087	<i>LOC283587</i>	Hypothetical protein
50615	<i>HSPA1L</i>	Heat shock 70-kd protein 1-like
767721	<i>FLJ32810</i>	Hypothetical protein
159470	<i>SPTAN1</i>	Spectrin, α , nonerythrocytic 1 (α -fodrin)
1159963	<i>IRF7</i>	Interferon regulatory factor 7
380890	<i>FLJ20202</i>	Hypothetical protein
377048	<i>MYO1B</i>	Myosin 1B
151501	<i>TEK</i>	TEK tyrosine kinase, endothelial
773183	<i>GTL3</i>	Likely ortholog of mouse gene trap locus 3

* Significance was defined as $q < 0.012$. EGF = endothelial growth factor; TEK = tunica interna endothelial cell kinase.

pattern of Cyr61 in RA synovial tissue, with overexpression in macrophages and lining cells, suggests that this protein plays a role in RA pathogenesis.

Immunohistochemical analysis did not reveal significant Cyr61 staining in synovial tissue lymphocytes. However, we reasoned that both the low abundance of B cells in the synovial tissue and the lack of distinguishing morphologic features that could be used to positively identify B cells could have prevented the detection of occasional Cyr61-positive synovial tissue B cells. To more directly determine whether synovial tissue B cells express Cyr61, double immunofluorescence analyses were performed using B cell-specific anti-CD20 and anti-Cyr61 antibodies. CD20-positive B cells were only sparsely present in human synovial tissue, but ~50% of

them showed Cyr61 protein expression (Figure 2C), indicating that some synovial tissue B cells do produce Cyr61 in situ.

The results of immunohistochemical analysis of 11 β -HSD2 protein expression are shown in Figure 3A. As can be seen in Figure 3B, similar to the results of Cyr61 immunostaining, 11 β -HSD2 showed higher immunoreactivity in macrophages of both OA (mean \pm SEM staining score 1.9 ± 0.3) and RA (staining score 2.4 ± 0.3) synovial tissue as compared with normal synovial tissue (0.8 ± 0.2 ; $P = 7.3 \times 10^{-4}$ and 2.6×10^{-4} , respectively). There was no significant difference between RA and OA 11 β -HSD2 macrophage immunostaining. Significantly increased immunostaining of 11 β -HSD2 was also found in smooth muscle cells of RA

Table 2. Selected functional classes defined by gene ontology, for genes with significantly higher messenger RNA expression in twins with rheumatoid arthritis compared with their healthy cotwins

Class, image no.	Gene	Title*	q value
Cell death			
754200	<i>BOK</i>	BCL2-related ovarian killer	0.025
83210	<i>C8B</i>	Complement component 8, β polypeptide	0.034
109863	<i>EMP2</i>	Epithelial membrane protein 2	0.018
811900	<i>LTBR</i>	Lymphotoxin β receptor (TNFR superfamily, member 3)	0.012
125308	<i>MPO</i>	Myeloperoxidase	0.043
132690	<i>PDCD4</i>	Programmed cell death 4	0.043
115337	<i>PRKCE</i>	Protein kinase C, ϵ	0.039
380620	<i>PSEN2</i>	Presenilin 2 (Alzheimer disease 4)	0.028
322051	<i>PTH</i>	Parathyroid hormone	0.031
781222	<i>TIAF1</i>	TGF β 1-induced antiapoptotic factor 1	0.018
Immune response			
2514098	<i>ARL6IP2</i>	ADP-ribosylation factor-like 6 interacting protein 2	0.022
83210	<i>C8B</i>	Complement component 8, β polypeptide	0.034
80948	<i>IGJ</i>	Immunoglobulin J polypeptide, linker protein for immunoglobulin α and μ polypeptides	0.043
840460	<i>IL7R</i>	Interleukin-7 receptor	0.031
811900	<i>LTBR</i>	Lymphotoxin β receptor (TNFR superfamily, member 3)	0.012
418422	<i>PPBP</i>	Proplatelet basic protein (chemokine [C-X-C motif], ligand 7)	0.043
215000	<i>VIPR1</i>	Vasoactive intestinal peptide receptor 1	0.045
Proteolysis and peptidolysis			
359285	<i>CPA4</i>	Carboxypeptidase A4	0.012
767642	<i>FLJ90650</i>	Laeverin	0.012
324220	<i>FBXO6</i>	F-box only protein 6	0.043
41650	<i>HGF</i>	Hepatocyte growth factor (hepapoietin A, scatter factor)	0.034
731330	<i>PLAU</i>	Plasminogen activator, urokinase	0.028
307687	<i>PRSS16</i>	Protease, serine 16 (thymus)	0.040
376080	<i>XPNPEP2</i>	X-prolyl aminopeptidase 2, membrane-bound	0.040
Heat-shock protein activity			
811813	<i>HSPA1B</i>	Heat shock 70-kd protein 1B	0.012
503555	<i>HSPA4</i>	Heat shock 70-kd protein 4	0.031
Chemokine activity			
324437	<i>CXCL1</i>	Chemokine (C-X-C motif) ligand 1	0.014
768561	<i>CCL2</i>	Chemokine (C-C motif) ligand 2	0.034
784337	<i>CXCL12</i>	Chemokine (C-X-C motif) ligand 12	0.039
418422	<i>PPBP</i>	Chemokine (C-X-C motif) ligand 7	0.043
247281	<i>CCR6</i>	Chemokine (C-C motif) receptor 6	0.034
Cell-cell signaling			
124014	<i>AGT</i>	Angiotensinogen	0.023
40338	<i>CNTNAP2</i>	Contactin-associated protein-like 2	0.028
46518	<i>DTNA</i>	Dystrobrevin, α	0.022
50930	<i>FGF12</i>	Fibroblast growth factor 12	0.031
434768	<i>FST</i>	Follistatin	0.022
415145	<i>HSD11B2</i>	β -hydroxysteroid dehydrogenase 2	0.012
795398	<i>PCDHB16</i>	Protocadherin β 16	0.037
322051	<i>PTH</i>	Parathyroid hormone	0.031
215000	<i>VIPR1</i>	Vasoactive intestinal peptide receptor 1	0.045
Transcription factor activity			
815287	<i>BRD8</i>	Bromo domain-containing 8	0.028
279482	<i>FOXP1</i>	Forkhead box P1	0.031
300866	<i>HOXC6</i>	Homeobox C6	0.049
594556	<i>MTA3</i>	Metastasis-associated family, member 3	0.045
782824	<i>MTF1</i>	Metal-regulatory transcription factor 1	0.043
289447	<i>POU6F1</i>	POU domain, class 6, transcription factor 1	0.028
773322	<i>SHOX2</i>	Short stature homeobox 2	0.028
840636	<i>SRF</i>	Serum response factor	0.053
135673	<i>STI8</i>	Suppression of tumorigenicity 18	0.028
397488	<i>TBX3</i>	T-box 3 (ulnar mammary syndrome)	0.037
364555	<i>THRB</i>	Thyroid hormone receptor, β	0.022
784035	<i>UBP1</i>	Upstream binding protein 1 (LBP-1a)	0.037
80384	<i>VAV1</i>	Vav 1 oncogene	0.043
668182	<i>ZNF193</i>	Zinc finger protein 193	0.053
296429	<i>ZNF24</i>	Zinc finger protein 24 (KOX 17)	0.049

Table 2. (Cont'd)

Class, image no.	Gene	Title	q value
738912	<i>ZNF323</i>	Zinc finger protein 323	0.039
562115	<i>ZNF36</i>	Zinc finger protein 36 (KOX 18)	0.049
G-protein-coupled receptor activity			
247281	<i>CCR6</i>	Chemokine (C-C motif) receptor 6	0.034
215000	<i>VIPRI</i>	Vasoactive intestinal peptide receptor 1	0.045
Cell motility			
789011	<i>AAMP</i>	Angio-associated, migratory cell protein	0.022
344091	<i>CACNG1</i>	Calcium channel, voltage-dependent, γ -subunit 1	0.053
247281	<i>CCR6</i>	Chemokine (C-C motif) receptor 6	0.034
486787	<i>CNN3</i>	Calponin 3, acidic	0.045
46518	<i>DTNA</i>	Dystrobrevin, α	0.022
119133	<i>MAPK8</i>	Mitogen-activated protein kinase 8	0.053
142556	<i>PSG2</i>	Pregnancy-specific β_1 -glycoprotein 2	0.022
845477	<i>PTGS2</i>	Prostaglandin-endoperoxide synthase 2	0.028
754358	<i>SPOCK</i>	Sparc/osteonectin, cwcv and kazal-like domains, proteoglycan (testican)	0.031
788695	<i>TNNT3</i>	Troponin T3, skeletal, fast	0.045
823932	<i>TPM1</i>	Tropomyosin 1 (α)	0.018
215000	<i>VIPRI</i>	Vasoactive intestinal peptide receptor 1	0.045

* BCL2 = β cell leukemia 2; TNFR = tumor necrosis factor receptor; TGF β 1 = transforming growth factor β 1; POU = Pit-1, Oct-1 and Oct-2, one-86; LBP-1a = leader binding protein 1a.

synovial tissue and OA synovial tissue as compared with normal synovial tissue. In contrast to Cyr61 immunostaining, 11 β -HSD2 expression in lining cells was comparable among all 3 groups. Endothelial cells in RA synovial tissue showed higher 11 β -HSD2 immunoreactivity compared with normal synovial tissue ($P = 0.031$), underscoring the potential role of this molecule in the angiogenic process in RA synovium. Similar to Cyr61 immunostaining, 11 β -HSD2 immunoreactivity in synovial tissue fibroblasts was markedly lower in RA than in OA or normal synovial tissue (Figure 3B). Thus, the results shown in Figures 2 and 3 demonstrate a nonrandom and lineage-selective immunoreactivity to Cyr61 and 11 β -HSD2 in RA synovial tissue.

The immunostaining results in OA synovial tissue suggest that expression of these 2 proteins may correlate with the extent of inflammatory changes or vascularity, which are 2 parameters that can be increased in OA synovial tissue (16). To quantify these parameters, inflammation and vascularity scores were determined in each of the normal, OA, and RA groups (Figures 3C and D). The abundance of inflammatory cells was significantly higher in OA synovial tissue (mean \pm SEM inflammation score 0.9 ± 0.2) compared with normal synovial tissue (inflammation score 0.1 ± 0.1) ($P = 1.7 \times 10^{-5}$) and was higher in RA synovial tissue (inflammation score 3.0 ± 0.2) compared with normal synovial tissue ($P = 7.4 \times 10^{-12}$). Both the OA and the RA group also showed a significant increase in synovial

tissue vascularity (mean \pm SEM vascularity score 2.9 ± 0.3 and 3.1 ± 0.1 , respectively) as compared with normal tissue (vascularity score 1.8 ± 0.1) ($P = 2 \times 10^{-6}$ or 9.7×10^{-8} , respectively).

Of interest, Cyr61 protein expression on synovial tissue macrophages positively correlated with the inflammation score in RA, OA, and normal synovial tissue (total of 46 samples; $r = 0.72$, $P = 1.5 \times 10^{-8}$), suggesting that Cyr61 may be a useful marker of the inflammatory process in arthritis. Similarly, 11 β -HSD2 immunostaining of synovial tissue macrophages showed a positive correlation with the level of inflammation in synovial tissue (total of 34 samples; $r = 0.61$, $P = 0.001$). Thus, the expression levels of Cyr61 and 11 β -HSD2 in synovial tissue may reflect the extent of inflammation and vascularity.

The product of the most significantly overexpressed gene, *FLJ90650*, has been recently identified as laeverin. To date, this N-aminopeptidase has been detected in human placenta only (15). Given its highly significant overexpression in the RA LCLs, we sought to investigate its expression in synovial tissue. In the absence of laeverin-specific antibodies, we used a real-time PCR approach to quantify its expression levels. As shown in Figure 4, RA synovial tissue ($n = 14$) displayed markedly higher levels of laeverin mRNA transcripts as compared with those displayed by OA synovial tissue ($n = 9$) ($P = 0.006$).

Table 3. Selected functional classes, by gene ontology, for genes with significantly lower messenger RNA expression in twins with rheumatoid arthritis compared with their healthy cotwins

Class, image no.	Gene	Title*	q value
Cell death			
202682	<i>C8A</i>	Complement component 8, α -polypeptide	0.014
72778	<i>CASP7</i>	Caspase 7, apoptosis-related cysteine protease	0.031
344272	<i>EMP3</i>	Epithelial membrane protein 3	0.028
773724	<i>FADD</i>	Fas (TNFRSF6)-associated via death domain	0.039
85195	<i>GADD45G</i>	Growth arrest and DNA-damage-inducible, γ	0.045
345232	<i>LTA</i>	Lymphotoxin α (TNFSF, member 1)	0.049
469954	<i>PRKCA</i>	Protein kinase C, α	0.045
592125	<i>RIPK1</i>	Receptor (TNFRSF)-interacting serine-threonine kinase 1	0.014
270917	<i>SFRP1</i>	Secreted frizzled-related protein 1	0.028
136821	<i>TGFB1</i>	Transforming growth factor β 1	0.039
489519	<i>TIMP3</i>	Tissue inhibitor of metalloproteinases 3	0.023
665356	<i>TNFRSF11B</i>	TNFRSF member 11b	0.028
Immune response			
878798	<i>B2M</i>	β_2 -microglobulin	0.037
202682	<i>C8A</i>	Complement component 8, α -polypeptide	0.014
295866	<i>CD74</i>	CD74 antigen	0.043
742132	<i>GIP2</i>	Interferon- α -inducible protein (clone IFI-15K)	0.028
233583	<i>IL1R2</i>	Interleukin-1 receptor, type II	0.049
345232	<i>LTA</i>	Lymphotoxin α (TNFSF, member 1)	0.049
Proteolysis and peptidolysis			
72778	<i>CASP7</i>	Caspase 7, apoptosis-related cysteine protease	0.031
141623	<i>LAP3</i>	Leucine aminopeptidase 3	0.045
489519	<i>TIMP3</i>	Tissue inhibitor of metalloproteinases 3	0.023
34010	<i>UQCRC2</i>	Ubiquinol-cytochrome c reductase core protein II	0.040
Heat-shock protein activity			
810053	<i>DNAJB2</i>	DnaJ (heat shock protein 40) homolog, subfamily B, member 2	0.014
299517	<i>DYT1</i>	Dystonia 1, torsin (autosomal dominant; torsin A)	0.039
50615	<i>HSPA1L</i>	Heat shock 70-kd protein 1-like	0.012
247816	<i>C5</i>	Complement component 5	0.049
Cell-cell signaling			
774446	<i>ADM</i>	Adrenomedullin	0.049
47204	<i>CPNE6</i>	Copine VI (neuronal)	0.039
742132	<i>GIP2</i>	Interferon- α -inducible protein (clone IFI-15K)	0.028
878838	<i>GRM3</i>	Glutamate receptor, metabotropic 3	0.025
40608	<i>HCRTR1</i>	Hypocretin (orexin) receptor 1	0.014
345232	<i>LTA</i>	Lymphotoxin α (TNFSF member 1)	0.049
784959	<i>NEO1</i>	Neogenin homolog 1 (chicken)	0.031
136821	<i>TGFB1</i>	Transforming growth factor β 1	0.039
774446	<i>ADM</i>	Adrenomedullin	0.049
Transcription factor activity			
595078	<i>BHLHB3</i>	Basic helix-loop-helix domain-containing, class B, 3	0.043
260303	<i>ETS2</i>	v-ets erythroblastosis virus E26 oncogene homolog 2	0.039
767183	<i>HCLS1</i>	Hematopoietic cell-specific Lyn substrate 1	0.025
611075	<i>HOXA1</i>	Homeobox A1	0.037
1155071	<i>HOXA5</i>	Homeobox A5	0.023
1159963	<i>IRF7</i>	Interferon regulatory factor 7	0.012
46561	<i>LZTS1</i>	Leucine zipper, putative tumor suppressor 1	0.014
299468	<i>NR2C2</i>	Nuclear receptor subfamily 2, group C, member 2	0.043
897575	<i>PCQAP</i>	PC2 glutamine/Q-rich-associated	0.028
769571	<i>SREBF1</i>	Sterol regulatory element binding	0.014
713839	<i>TFAP4</i>	Transcription factor AP-4	0.034
824074	<i>YY1</i>	YY1 transcription factor	0.037
G protein-coupled receptor activity			
22411	<i>FY</i>	Duffy blood group	0.031
878838	<i>GRM3</i>	Glutamate receptor, metabotropic 3	0.025
40608	<i>HCRTR1</i>	Hypocretin (orexin) receptor 1	0.014
490434	<i>LGR7</i>	Leucine-rich repeat-containing G protein-coupled receptor	0.045
33045	<i>NPY1R</i>	Neuropeptide Y receptor Y1	0.039
Cell motility			
813179	<i>IGF1</i>	Insulin-like growth factor 1 (somatomedin C)	0.049
810947	<i>MYH11</i>	Myosin, heavy polypeptide 11, smooth muscle	0.043
784959	<i>NEO1</i>	Neogenin homolog 1 (chicken)	0.031
773771	<i>PLN</i>	Phospholamban	0.040
33511	<i>SLMAP</i>	Sarcolemma-associated protein	0.012
589869	<i>TAZ</i>	Tafazzin	0.037

* TNFRSF6 = tumor necrosis factor receptor superfamily 6; PC2 = protein complex 2; AP-4 = activator protein 4.

DISCUSSION

Using cDNA microarray analyses of LCLs derived from 11 pairs of RA-discordant MZ twins, we identified a group of disease-relevant, differentially expressed genes. Gene ontology analysis provided a biologic context for these genes. The disease relevance of the products of the 3 most significantly overexpressed genes, not previously known to be involved in RA pathogenesis, was further suggested by direct demonstration of their abundance in the synovium.

This is the first report of the use of microarray gene expression analysis in MZ twins in RA. To date, research efforts to characterize the molecular events contributing to RA pathogenesis by gene microarray analysis have focused on the rheumatoid pannus, using a case-control approach (17–20). However, interpretation of these studies is confounded by the use of unrelated RA patients with heterogeneous genetic backgrounds, in addition to unavoidable microheterogeneity within the synovial tissue itself. We compared the results from our data set with those from the public microarray data set (17) but could find no significant concordance between the 2 sets of results. The advantage of our approach is that it allows comparisons with genetically identical normal controls, thereby examining RA-specific, disease-modulated transcripts. Thus, this approach offers a focused analysis of genes modulated by nonhereditary mechanisms, which play a major role in triggering onset of disease in genetically susceptible individuals, as has been suggested in analyses of twin RA concordance rates (5).

DNA microarray analyses of MZ twin samples have been previously used to identify disease mechanisms in only 3 studies (21–23), and have never been used in RA before. Twin microarray analysis has been found to be a useful investigative tool in 2 hematologic malignancies (21,22) and in 1 nonmalignant condition (23). Using DNA microarray analysis of LCLs derived from 2 pairs of twins discordant for bipolar disorder, Kakiuchi et al recently discovered that down-regulation of genes related to the stress response plays a role in the pathogenesis of that disorder (23). It is noteworthy that the extent of heterogeneity in gene expression detected by microarray between affected and nonaffected MZ twin pairs is remarkably low (24). The observation that there is low background “noise” with this method makes microarray analysis of disease-discordant MZ twin pairs a particularly powerful investigative tool.

To overcome the scarcity of peripheral blood B cells in RA (25,26) we used immortalized lymphoblastoid B cell lines. It is intriguing that stable differences

could be seen in long-term-cultured LCLs. It should be added, however, that long-term LCLs have been previously found to exhibit lasting phenotypic and functional traits in at least 16 other diseases, both immune-mediated and non-immune-mediated (a complete list of the representative diseases studied with LCLs can be obtained from the authors). As an example, long-term LCLs of individuals with bipolar disorder display altered signal transduction systems (27,28) and down-regulated expression of stress response genes (23). Similarly, stable disease-specific aberrations were found in long-term LCLs from patients with diverse metabolic, vascular, neoplastic, and hematologic disorders. Using both case-control and MZ twin analyses, we recently documented long-lasting increased mRNA expression and enzymatic activity of sphingosine kinase 1 (SphK1) in LCLs from RA patients compared with healthy controls (29).

The extent to which the *in vitro* immortalized LCLs faithfully represent the pool of peripheral blood B cells is presently unknown. However, using a double-staining immunofluorescence technique, we were able to demonstrate expression of Cyr61 synovial tissue B cells. Approximately 50% of synovial tissue CD20-positive cells expressed this protein. It should be mentioned that since Cyr61 is a secreted protein, the actual percentage of B cells producing this protein could be higher than 50%. Our immunohistochemistry data indicated that products of the top-ranked genes found to be overexpressed in LCLs by microarray analysis were also expressed in nonlymphoid synovial tissue cells. It has been previously noted that LCLs can display phenotypic and functional aberrations commonly assumed to be restricted to nonlymphoid tissues. For example, LCLs have been previously used to study the mechanism of endothelial abnormalities in hypertension, platelet defects in Glanzmann thrombasthenia, cytoskeletal aberrations in Wiskott-Aldrich syndrome, multisystemic glycosylation defects in carbohydrate-deficient glycoprotein syndrome IA, defective granulocyte NADPH oxidase activity in chronic granulomatous disease, and neuronal abnormalities in bipolar disorder, to mention only a few conditions. Thus, ectopic expression by the LCLs in terms of its association with pathologic development is not without precedence.

The mechanisms that allow LCLs to express ectopic phenotypes and to maintain this aberration in long-term culture are presently unknown, although the phenomenon has long been recognized as illegitimate transcription (30). One potential explanation could be EBV-induced differential DNA methylation. It has been previously found that EBV transformation involves profound DNA methylation changes (31). It is noteworthy

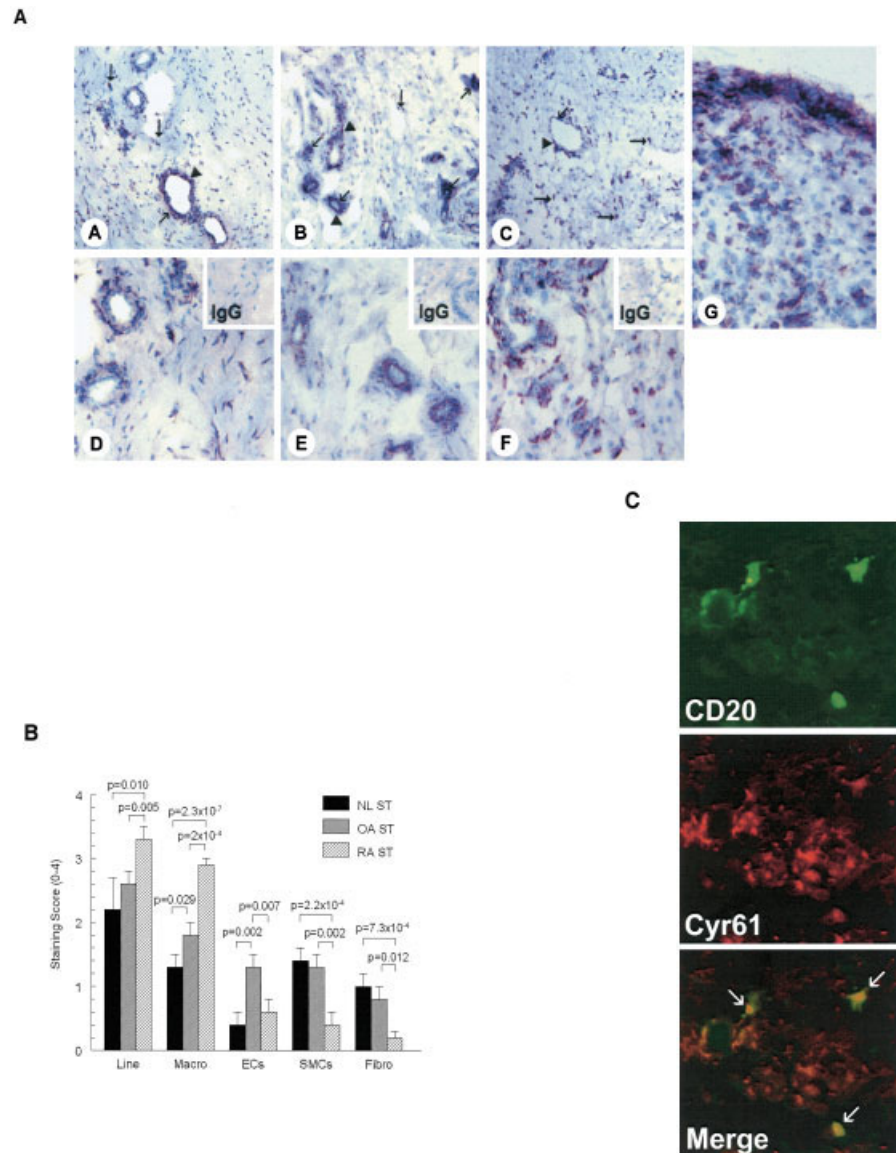


Figure 2. Expression patterns of cysteine-rich, angiogenic inducer 61 (Cyr61) in normal (NL), osteoarthritis (OA), and rheumatoid arthritis (RA) synovial tissue (ST). **A**, Representative ST sections demonstrating Cyr61 immunostaining on normal (panels **A** and **D**), OA (panels **B** and **E**), and RA (panels **C**, **F**, and **G**) ST. Rabbit IgG was used as a negative control (inserts in panels **D**, **E**, and **F**). Cyr61 expression on macrophages (**solid arrows**) showed low constitutive staining in normal ST but was up-regulated in both OA and RA ST. Cyr61 expression on endothelial cells (**open arrows**) was most notably seen in OA ST, while immunopositivity on smooth muscle cells (**arrowheads**) was decreased in RA ST. Intense Cyr61 staining was observed on ST lining cells of RA patients (panel **G**) but also in the synovial lining of normal and OA subjects (not shown) (original magnification $\times 200$ in panels **A**, **B**, and **C**; $\times 400$ in panels **D**, **E**, **F**, and **G**). **B**, Quantification of the expression pattern of Cyr61 in distinct cells from normal subjects ($n = 16$), OA patients ($n = 16$), and RA patients ($n = 14$). Data are the mean and SEM. Staining was quantified in synovial lining cells (Line), macrophages (Macro), endothelial cells (ECs), smooth muscle cells (SMCs), and synovial fibroblasts (Fibro). In RA ST, Cyr61 expression was significantly ($P < 0.05$) higher on lining cells and macrophages but decreased on smooth muscle cells and fibroblasts as compared with normal and OA ST. Cyr61 immunopositivity on endothelial cells was comparable in normal and RA ST, but increased in OA ST. **C**, Immunofluorescence costaining with the B cell marker CD20 and Cyr61 on human ST. Occasional CD20-positive B cells (green) were detected. Costaining with an anti-Cyr61 antibody (red) revealed colocalization in some B cells after merging (**arrows**) (original magnification $\times 400$).

that differential DNA methylation profiles have been shown to spontaneously exist in MZ twins (32) and have been implicated in the pathogenesis of autoimmune

diseases, including RA (33). Given these observations and the long-hypothesized role of EBV in RA etiology (for review, see ref. 34), it is tempting to speculate that

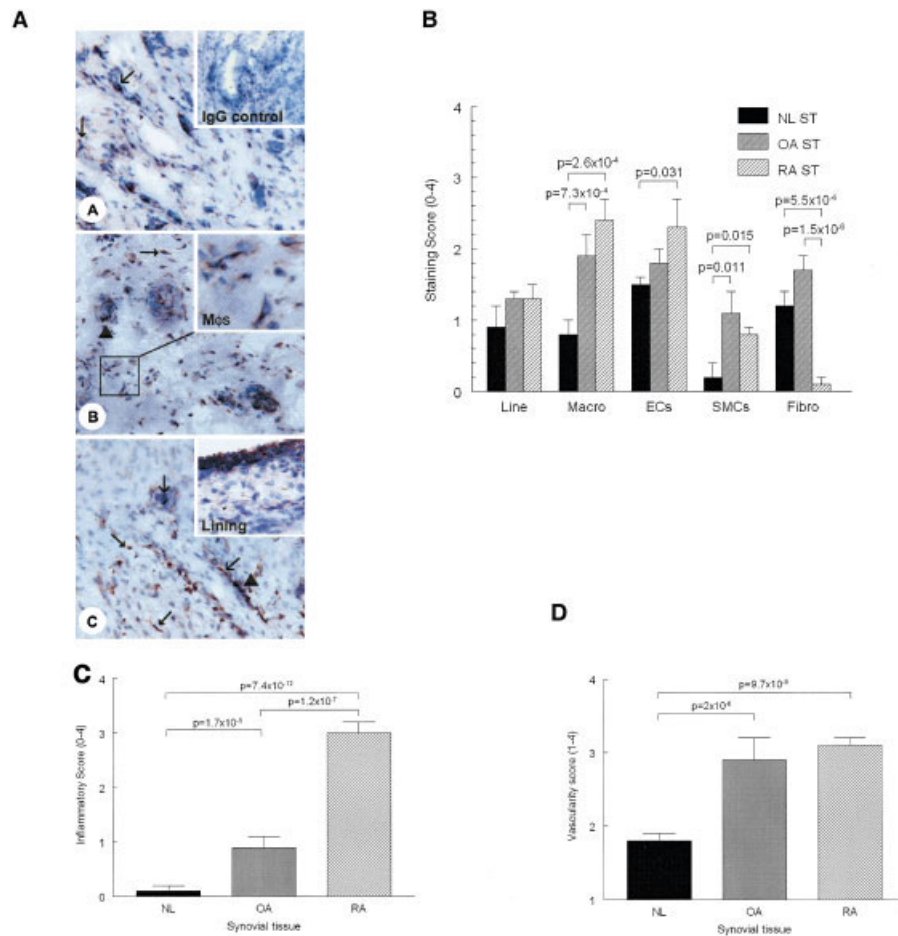


Figure 3. Expression patterns of 11 β -hydroxysteroid dehydrogenase type 2 (11 β -HSD2) in normal, OA, and RA ST. **A**, Representative immunohistochemistry showing 11 β -HSD2 expression in normal, OA, and RA ST (panels **A**, **B**, and **C**, respectively) as compared with IgG control (insert in panel **A**). Staining for macrophages (M Φ s) (solid arrows) (insert in panel **B**) was weakly positive in normal ST, and more prominent in OA ST and RA ST. Open arrows denote positive staining in endothelial cells, showing increased expression on RA ST. Arrowheads indicate immunoreactivity in smooth muscle cells. Comparable positive staining was also seen in lining cells (Lining) (insert in panel **C**) in all 3 groups (original magnification \times 400). **B**, Quantification of the expression pattern of 11 β -HSD2 in distinct cells in STs from normal subjects ($n = 13$), OA patients ($n = 12$), and RA patients ($n = 13$). Immunopositivity for 11 β -HSD2 on macrophages and smooth muscle cells was significantly higher in OA and RA ST compared with normal ST. Expression of 11 β -HSD2 on endothelial cells was also significantly higher in RA ST ($P = 0.031$), while immunopositivity in RA ST fibroblasts was decreased. **C**, Histologic inflammation score in STs from normal subjects ($n = 13$), OA patients ($n = 12$), and RA patients ($n = 9$). The inflammation score was significantly higher in OA ST compared with normal ST, while RA ST showed even more inflammatory cell influx. **D**, Histologic vascularity score in STs from normal subjects ($n = 13$), OA patients ($n = 12$), and RA patients ($n = 9$). Vascularity in RA and OA ST was significantly higher than in normal ST. Values in **B**, **C**, and **D** are the mean and SEM. See Figure 2 for other definitions.

the virus could amplify subtle, preexisting methylation disparities. In any event, our data clearly indicate that whatever changes may have occurred as a result of in vitro B cell transformation, these changes had a differential effect in the healthy twins compared with the RA twins, in a highly statistically significant and pathogenically consistent manner, thus highlighting a fundamental biologic aberration in RA.

Gene ontology analyses revealed that many RA-

related genes were differentially expressed in LCLs. Although the enrichment differences did not reach statistically significant levels, this does not diminish the biologic relevance of the findings, since it may take only a few aberrantly expressed genes to produce a pathogenic result. Given our findings of SphK1-mediated impairment of Fas-mediated cell death signaling in RA LCLs (29), it is intriguing that in the present study, gene ontology analysis revealed that many of the disparately

expressed genes in LCLs belonged to the cell death machinery (Tables 2 and 3). For instance, whereas the proapoptotic genes for caspase 7 (*CASP7*), Fas-associated via death domain (*FADD*), and tumor necrosis factor receptor superfamily member 11b (*TNFRSF11B*) were down-regulated, the antiapoptotic gene for transforming growth factor β 1-induced antiapoptotic factor 1 (*TIAF1*), a B cell leukemia 2-related gene (*BOK*), and a lymphotoxin- β receptor gene (*LTBR*) were overexpressed (Table 2). Thus, microarray analysis of LCLs revealed a tightly coordinated apoptosis-related gene expression profile.

Gene ontology analysis also revealed coordinated expression profiles in genes associated with immune response, including innate immunity-related genes. For example, proinflammatory genes such as those for interleukin-7 receptor (*IL7R*) and *LTBR* were overexpressed, while *CD74*, IL-1 receptor type II (*IL1R2*), interferon- α -inducible protein (*GIP2*), and lymphotoxin- α (*LTA*) were underexpressed in the RA twins. An interesting reciprocal expression pattern was found with the α - and β -chains of the complement component 8 (C8) β -chain (*C8B*), in which the β -chain was found to be overexpressed while the α -chain (*C8A*) was underexpressed. Analogously, while *LTBR* was overexpressed in RA twins, *LTA* and *TNFRSF11B* were overexpressed in the healthy cotwins. A reciprocal relationship was also found in the expression profiles of heat-shock proteins: heat shock 70-kd proteins 1B (*HSPA1B*) and 4 (*HSPA4*) were overexpressed in the RA twins, while heat shock 70-kd protein 1-like (*HSPAIL*) was underexpressed,

consistent with recent evidence that heat-shock proteins may modulate the course of RA (35).

In the chemokine genes category, 4 genes that encode chemokines, and one that encodes a chemokine receptor, were overexpressed (Table 2). All 5 of these genes and/or their products have been previously reported to be overexpressed in RA. For example, the CXCL1 protein (also known as GRO α), which is implicated in ingress of inflammatory cells into the synovium in RA, is overexpressed in RA synovial tissue lining cells and subsynovial tissue macrophages, as well as in plasma, synovial fluid, and synovial fluid cells of RA patients (36,37). Synovial fluid CCL2 and CXCL12 levels are increased and the proteins have been shown to chemoattract Th1 lymphocytes (38). PPBP (also known as CTAP-III) is a C-X-C-motif chemokine that has long been found in RA synovial fluid (39). CCR6 protein (40) and mRNA transcripts (41) have been demonstrated in RA synovial tissue. Thus, the panel of chemokine genes identified in the present study by an iterative approach corroborates many previous hypothesis-based studies that have implicated these genes individually in RA pathogenesis.

The gene ontology category of proteolysis and peptidolysis also revealed interesting coordinated expression profiles. The gene encoding the antiproteolytic protein for tissue inhibitor of metalloproteinases 3 (*TIMP3*) was underexpressed, whereas the propeptolytic genes for carboxypeptidase A4 (*CPA4*), plasminogen activator, urokinase (*PLAU*), serine protease 16 (*PRSS16*), X-prolyl aminopeptidase 2, membrane-bound (*XPNPEP2*), and the recently cloned gene *FLJ90650* (presently known to encode laeverin) were all overexpressed in RA LCLs.

FLJ90650 was found to be the most significantly overexpressed gene in RA twin LCLs. This gene, the product function of which has not been studied to date, was recently found to be expressed in human extravillous trophoblasts (15). Its predicted amino acid sequence suggests that it belongs to a group of membrane-bound gluzincin metalloproteinases and shows significant homology to aminopeptidase N (CD13), an enzyme involved in degradation of extracellular matrix, chemoattraction of T lymphocytes, and antigen processing by antigen-presenting cells (42,43). CD13 has been shown to play a functional role in RA (44). Our findings provide the first evidence that laeverin, a newly discovered aminopeptidase, is abundantly expressed in RA synovial tissue.

The second most significantly overexpressed gene in RA LCLs was *HSD11B2*, which encodes 11 β -HSD2, a

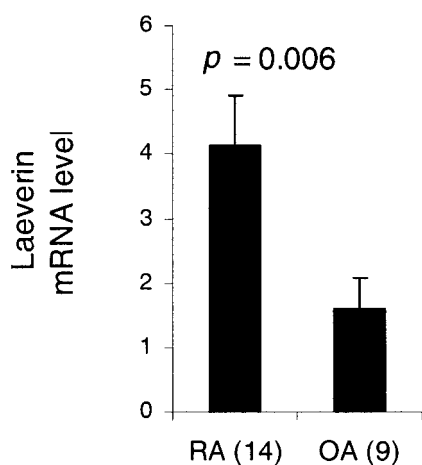


Figure 4. Real-time polymerase chain reaction analysis of laeverin mRNA expression levels in synovial tissue from 14 patients with rheumatoid arthritis (RA) and 9 patients with osteoarthritis (OA). Bars show the mean and SEM.

dehydrogenase that converts active glucocorticoids (cortisol and corticosterone) into inactive 11-ketosteroids. Similar to laeverin, 11 β -HSD2 protein was found to be abundantly expressed in synovial tissues; however, 11 β -HSD2 has not previously been directly implicated in RA. However, several of its characteristics make it a likely participant in the pathogenesis of this disease. For example, this enzyme can cause resistance to glucocorticoids (45), an aberration that has been previously reported in RA (46). Increasing tissue availability of glucocorticoids by an 11 β -HSD inhibitor has been shown to have a therapeutic effect in MRL-*lpr/lpr* mice (47). In addition, 11 β -HSD2 has been implicated in the disequilibrium between the positive and negative effect of glucocorticoids on bone, which leads to osteoporosis (48), a common finding in the periarticular bone in RA. In this context it should be pointed out that another osteoporosis-associated gene, osteoclast stimulating factor 1 (*OSTF1*), was identified as one of the most significantly overexpressed genes (Table 2), while osteoprotegerin (*TNFRSF11B*), an antiosteoporosis molecule, was found to be underexpressed in the RA twin LCLs (Table 3).

CYR61 was the third most significantly overexpressed gene in RA twin LCLs. We demonstrated abundant expression of the gene product in the synovium by immunohistochemistry. This protein has never been directly implicated in RA. However, given the central role of angiogenesis in the pathogenesis of RA pannus (3), Cyr61, a well-established angiogenic factor, is a likely culprit. The gene encoding Cyr61 has been previously shown to be overexpressed in other active inflammatory conditions, such as hyperoxic lung injury (49) or early Graves' ophthalmopathy, in which it was proposed as a marker of disease activity (50).

In summary, we report herein a novel approach for identification of potential disease-relevant genes in RA, using LCLs from disease-discordant MZ twins. Although the pathogenic role of the newly reported genes remains to be determined, the representation of many established pannus-associated genes in this analysis suggests that this approach could provide mechanistic insights into the pathogenesis of RA and could help identify novel candidate targets for therapeutic intervention.

ACKNOWLEDGMENTS

We thank Michael Hayes and Rita Martinez for technical assistance.

REFERENCES

1. Firestein GS. Evolving concepts of rheumatoid arthritis. *Nature* 2003;423:356–61.
2. Liu H, Pope RM. Apoptosis in rheumatoid arthritis: friend or foe. *Rheum Dis Clin North Am* 2004;30:603–25.
3. Szekanecz Z, Gaspar L, Koch AE. Angiogenesis in rheumatoid arthritis. *Front Biosci* 2005;10:1739–53.
4. Goronzy JJ, Weyand CM. Rheumatoid arthritis. *Immunol Rev* 2005;204:55–73.
5. Silman AJ, MacGregor AJ, Thomson W, Holligan S, Carthy D, Farhan A, et al. Twin concordance rates for rheumatoid arthritis: results from a nationwide study. *Br J Rheumatol* 1993;32:903–7.
6. Tosato G. Generation of Epstein-Barr virus (EBV)-immortalized B cell lines. In: Coligan JE, Kruisbeek AM, Margulies DH, Shevach EM, Strober W, editors. *Current protocols in immunology*. New York: John Wiley & Sons; 1998. p. 7.22.1–7.22.3.
7. Arnett FC, Edworthy SM, Bloch DA, McShane DJ, Fries JF, Cooper NS, et al. The American Rheumatism Association 1987 revised criteria for the classification of rheumatoid arthritis. *Arthritis Rheum* 1988;31:315–24.
8. Altman R, Alarcon G, Appelrouth D, Bloch D, Borenstein D, Brandt K, et al. The American College of Rheumatology criteria for the classification and reporting of osteoarthritis of the hip. *Arthritis Rheum* 1991;34:505–14.
9. Dhanasekaran SM, Barrette TR, Ghosh D, Shah R, Varambally S, Kurachi K, et al. Delineation of prognostic biomarkers in prostate cancer. *Nature* 2001;412:822–6.
10. Tusher VG, Tibshirani R, Chu G. Significance analysis of microarrays applied to the ionizing radiation response. *Proc Natl Acad Sci U S A* 2001;98:5116–21.
11. Eisen MB, Spellman PT, Brown PO, Botstein D. Cluster analysis and display of genome-wide expression patterns. *Proc Natl Acad Sci U S A* 1998;95:14863–8.
12. Ashburner M, Ball CA, Blake JA, Botstein D, Butler H, Cherry JM, et al, and the Gene Ontology Consortium. Gene ontology: tool for the unification of biology. *Nat Genet* 2000;25:25–9.
13. Maglott DR, Katz KS, Sicotte H, Pruitt KD. NCBI's LocusLink and RefSeq. *Nucleic Acids Res* 2000;28:126–8.
14. Ruth JH, Volin MV, Haines GK 3rd, Woodruff DC, Katschke KJ Jr, Woods JM, et al. Fractalkine, a novel chemokine in rheumatoid arthritis and in rat adjuvant-induced arthritis. *Arthritis Rheum* 2001;44:1568–81.
15. Fujiwara H, Higuchi T, Yamada S, Hirano T, Sato Y, Nishioka Y, et al. Human extravillous trophoblasts express laeverin, a novel protein that belongs to membrane-bound gluzincin metalloproteinases. *Biochem Biophys Res Commun* 2004;313:962–8.
16. Haywood L, McWilliams DF, Pearson CI, Gill SE, Ganesan A, Wilson D, et al. Inflammation and angiogenesis in osteoarthritis. *Arthritis Rheum* 2003;48:2173–7.
17. Van der Pouw Kraan TC, van Gaalen FA, Kasperkovitz PV, Verbeet NL, Smeets TJ, Kraan MC, et al. Rheumatoid arthritis is a heterogeneous disease: evidence for differences in the activation of the STAT-1 pathway between rheumatoid tissues. *Arthritis Rheum* 2003;48:2132–45.
18. Zhang HG, Hyde K, Page GP, Brand JP, Zhou J, Yu S, et al. Novel tumor necrosis factor α -regulated genes in rheumatoid arthritis. *Arthritis Rheum* 2004;50:420–31.
19. Kasperkovitz PV, Timmer TC, Smeets TJ, Verbeet NL, Tak PP, van Baarsen LG, et al. Fibroblast-like synoviocytes derived from patients with rheumatoid arthritis show the imprint of synovial tissue heterogeneity: evidence of a link between an increased myofibroblast-like phenotype and high inflammation synovitis. *Arthritis Rheum* 2005 52:430–441.
20. Pierer M, Rethage J, Seibl R, Lauener R, Brentano F, Wagner U, et al. Chemokine secretion of rheumatoid arthritis synovial fibro-

- blasts stimulated by Toll-like receptor 2 ligands. *J Immunol* 2004;172:1256–65.
21. Munshi NC, Hideshima T, Carrasco D, Shamma M, Auclair D, Davies F, et al. Identification of genes modulated in multiple myeloma using genetically identical twin samples. *Blood* 2004;103:1799–806.
 22. Teuffel O, Betts DR, Dettling M, Schaub R, Schafer BW, Higgli FK. Prenatal origin of separate evolution of leukemia in identical twins. *Leukemia* 2004;18:1624–9.
 23. Kakiuchi C, Iwamoto K, Ishiwata M, Bundo M, Kasahara T, Kusumi I, et al. Impaired feedback regulation of XBP1 as a genetic risk factor for bipolar disorder. *Nat Genet* 2003;35:171–5.
 24. Tan Q, Christensen K, Christiansen L, Fredriksen H, Bathum L, Dahlgaard J, et al. Genetic dissection of gene expression observed in whole blood samples of elderly Danish twins. *Hum Genet* 2005;117:267–74.
 25. Wagner U, Kaltenhauser S, Pierer M, Wilke B, Arnold S, Hantzschel H. B lymphocytopenia in rheumatoid arthritis is associated with the DRB1 shared epitope and increased acute phase response. *Arthritis Res* 2002;4:R1.
 26. Symmons DP, Farr M, Salmon M, Bacon PA. Lymphopenia in rheumatoid arthritis. *J R Soc Med* 1989;82:462–3.
 27. Banks RE, Aiton JF, Cram G, Naylor GJ. Incorporation of inositol into the phosphoinositides of lymphoblastoid cell lines from bipolar manic-depressive patients. *J Affect Disord* 1990;19:1–8.
 28. Yoon IS, Li PP, Siu KP, Kennedy JL, Cooke RG, Parikh SV, et al. Altered IMPA2 gene expression and calcium homeostasis in bipolar disorder. *Mol Psychiatry* 2001;6:678–83.
 29. Pi X, Tan SY, Hayes M, Xiao L, Shayman JA, Ling S, et al. Sphingosine kinase 1-mediated inhibition of Fas death signaling in rheumatoid arthritis B lymphoblastoid cells. *Arthritis Rheum* 2006;54:754–64.
 30. Negrier C, Vinciguerra C, Attali O, Grenier C, Larcher ME, Dechavanne M. Illegitimate transcription: its use for studying genetic abnormalities in lymphoblastoid cells from patients with Glanzmann thrombasthenia. *Br J Haematol* 1998;100:33–9.
 31. Tao Q, Roberston KD. Stealth technology: how Epstein-Barr virus utilizes DNA methylation to cloak itself from immune detection. *Clin Immunol* 2003;109:53–63.
 32. Fraga MF, Ballestar E, Paz MF, Ropero S, Setien F, Ballestar ML, et al. Epigenetic differences arise during the lifetime of monozygotic twins. *Proc Natl Acad Sci U S A* 2005;102:10604–9.
 33. Richardson B, Scheinbart L, Strahler J, Gross L, Hanash S, Johnson M. Evidence for impaired T cell DNA methylation in systemic lupus erythematosus and rheumatoid arthritis. *Arthritis Rheum* 1990;33:1665–73.
 34. Sawada S, Takei M. Epstein-Barr virus etiology in rheumatoid synovitis. *Autoimmun Rev* 2005;4:106–10.
 35. Puga Yung GL, Le TD, Roord S, Prakken B, Albani S. Heat shock proteins for immunotherapy of rheumatoid arthritis. *Inflamm Res* 2003;52:443–51.
 36. Koch AE, Kunkel SL, Shah MR, Hosaka S, Halloran MM, Haines GK, et al. Growth-related gene product α : a chemotactic cytokine for neutrophils in rheumatoid arthritis. *J Immunol* 1995;155:3660–6.
 37. Konig A, Krenn V, Toksoy A, Gerhard N, Gillitzer R. Mig, GRO α and RANTES messenger RNA expression in lining layer, infiltrates and different leucocyte populations of synovial tissue from patients with rheumatoid arthritis, psoriatic arthritis and osteoarthritis. *Virchows Arch* 2000;436:449–58.
 38. Shadidi KR, Aarvak T, Henriksen JE, Natvig JB, Thompson KM. The chemokines CCL5, CCL2 and CXCL12 play significant roles in the migration of Th1 cells into rheumatoid synovial tissue. *Scand J Immunol* 2003;57:192–8.
 39. Myers SL, Christine TA. Measurement of β -thromboglobulin connective tissue activating peptide-III platelet antigen concentrations in pathologic synovial fluids. *J Rheumatol* 1982;9:6–12.
 40. Matsui T, Akahoshi T, Namai R, Hashimoto A, Kurihara Y, Rana M, et al. Selective recruitment of CCR6-expressing cells by increased production of MIP-3 α in rheumatoid arthritis. *Clin Exp Immunol* 2001;125:155–61.
 41. Ruth JH, Shahrara S, Park CC, Morel JC, Kumar P, Qin S, et al. Role of macrophage inflammatory protein-3 α and its ligand CCR6 in rheumatoid arthritis. *Lab Invest* 2003;83:579–88.
 42. Taki K, Ogushi F, Kawano T, Tada H, Hariguchi N, Sone S. CD13/aminopeptidase N: a novel chemoattractant for T lymphocytes in pulmonary sarcoidosis. *Am J Respir Crit Care Med* 2000;161:1–7.
 43. Hansen AS, Noren O, Sjostrom H, Werdelin O. A mouse aminopeptidase N is a marker for antigen-presenting cells and appears to be coexpressed with major histocompatibility complex class II molecules. *Eur J Immunol* 1993;23:2358–64.
 44. Shimizu T, Tani K, Hase K, Ogawa H, Huang L, Shinomiya F, et al. CD13/aminopeptidase N-induced lymphocyte involvement in inflamed joints of patients with rheumatoid arthritis. *Arthritis Rheum* 2002;46:2330–8.
 45. Sandeep TC, Walker BR. Pathophysiology of modulation of local glucocorticoid levels by 11 β -hydroxysteroid dehydrogenases. *Trends Endocrinol Metab* 2001;12:446–53.
 46. Lamberts SW, Huizenga AT, de Lange P, de Jong FH, Koper JW. Clinical aspects of glucocorticoid sensitivity. *Steroids* 1996;61:157–60.
 47. Horigome H, Hirano T, Oka K. Therapeutic effect of glycyrrhetic acid in MRL lpr/lpr mice: implications of alteration of corticosteroid metabolism. *Life Sci* 2001;69:2429–38.
 48. Cooper MS, Walker EA, Bland R, Fraser WD, Hewison M, Stewart PM. Expression and functional consequences of 11 β -hydroxysteroid dehydrogenase activity in human bone. *Bone* 2000;27:375–81.
 49. Perkowski S, Sun J, Singhal S, Santiago J, Leikauf GD, Albelda SM. Gene expression profiling of the early pulmonary response to hyperoxia in mice. *Am J Respir Cell Mol Biol* 2003;28:682–96.
 50. Lantz M, Vondrichova T, Parikh H, Frenander C, Ridderstrale M, Asman P, et al. Overexpression of immediate early genes in active Graves' ophthalmopathy. *J Clin Endocrinol Metab* 2005;90:4784–91.